
Adaptive Normalized Risk-Averting Training For Deep Neural Networks

Zhiguang Wang, Tim Oates

Department of Computer Science and Electrical Engineering

James Lo

Department of Mathematics and Statistics

University of Maryland Baltimore County

Baltimore, Maryland 21250

{stephen.wang, oates, jameslo}@umbc.edu

Abstract

This paper proposes a set of new error criteria and learning approaches, Adaptive Normalized Risk-Averting Training (ANRAT), to attack the non-convex optimization problem in training deep neural networks (DNNs). Theoretically, we demonstrate its effectiveness on global and local convexity lower-bounded by the standard L_p -norm error. By analyzing the gradient on the convexity index λ , we explain the reason why to learn λ adaptively using gradient descent works. In practice, we show how this method improves training of deep neural networks to solve visual recognition tasks on the MNIST and CIFAR-10 datasets. Without using pretraining or other tricks, we obtain results comparable or superior to those reported in recent literature on the same tasks using standard ConvNets + MSE/cross entropy. Performance on deep/shallow multilayer perceptrons and Denoised Auto-encoders is also explored. ANRAT can be combined with other quasi-Newton training methods, innovative network variants, regularization techniques and other specific tricks in DNNs. Other than unsupervised pretraining, it provides a new perspective to address the non-convex optimization problem in DNNs.

1 Introduction

Deep neural networks (DNNs) are attracting attention largely due to their impressive empirical performance in image and speech recognition tasks. While Convolutional Networks (ConvNets) are the de facto state-of-the-art for visual recognition, Deep Belief Networks (DBN), Deep Boltzmann Machines (DBM) and Stacked Auto-encoders (SA) provide insights as generative models to learn the full generating distribution of input data. Recently, researchers have investigated various techniques to improve the learning capacity of DNNs. Unsupervised pretraining using Restrict Boltzmann Machines (RBM), Denoised Autoencoders (DA) or Topographic ICA (TICA) has proved to be helpful for training DNNs with better weight initialization [1, 2]. Rectified Linear Unit (ReLU) and variants are proposed as the optimal activation functions to better interpret hidden features. Various regularization techniques such as dropout [3] with Maxout [4] are proposed to regulate the DNNs to be less prone to overfitting.

However, training deep multi-layered neural networks is known to be hard. Neural network models always lead to a non-convex optimization problem. The optimization algorithm impacts the quality of the local minimum because it is hard to find a global minimum or estimate how far a particular local minimum is from the best possible solution. The most standard approach to optimize DNNs is

Stochastic Gradient Descent (SGD). There are many variants of SGD and researchers and practitioners typically choose a particular variant empirically. While nearly all DNNs optimization algorithms in popular use are gradient-based, recent work has shown that more advanced second-order methods such as L-BFGS and Saddle-Free Newton (SFN) approaches can yield better results for DNN tasks [5, 6]. Although the high computational complexity of using second order derivatives can be addressed by hardware extensions (GPUs or clusters) or batch methods when dealing with massive data, SGD still provides a robust default choice for optimizing DNNs.

Instead of modifying the network structure or optimization techniques for DNNs, we focused on designing a new error function to convexify the error space. The convexification approach has been studied in the optimization community for decades, but has never been seriously applied within deep learning. Two well-known methods are the graduated nonconvexity method [7] and the LiuFloudas convexification method [8]. LiuFloudas convexification can be applied to optimization problems where the error criterion is twice continuously differentiable, although determining the weight α of the added quadratic function for convexifying the error criterion involves significant computation when dealing with massive data and parameters.

Following the same name employed for deriving robust controllers and filters [9], a new type of Risk-Averting Error (RAE) is proposed theoretically for solving non-convex optimization problems [10]. Empirically, with the proposal of Normalized Risk-Averting Error (NRAE) and the Gradual Deconvexification method (GDC), this error criterion is proved to be competitive with the standard mean square error (MSE) in single layer and two-layer neural networks for solving data fitting and classification problems [11, 12]. Interestingly, SimNets, a generalization of ConvNets that was recently proposed in [13], uses the MEX operator (whose name stands for Maximum-minimum-Expectation Collapsing Smooth) as an activation function to generalize ReLU activation and max pooling. We notice that the MEX operator with L_2 units has exactly the *same* mathematical form with NRAE.

However, NRAE is still hard to optimize in practice due to large plateaus and the unstable error space caused by the fixed large convexity index. GDC alleviates these problems but its performance is limited and suffers from the slow learning speed. This paper proposes a new set of training approaches, Adaptive Normalized Risk-Averting Training (ANRAT), to attack the non-convex optimization strategies in DNNs. We give theoretical proofs of its optimal properties against the standard L_p -norm error. Our experiments on MNIST and CIFAR-10 with different deep/shallow neural nets demonstrate the effectiveness empirically. Being an optimization algorithm, our approach are not supposed to deal specifically with the problem of over-fitting, however we show that this can be handled by the usual methods of regularization such as weight decay or dropout.

2 Convexification on Error Criterion

We begin with the definition of RAE for the L_p norm and the theoretical justifications on its convexity property. RAE is not suitable for real applications since it is not bounded. Instead, NRAE is bounded to overcome the register overflow in real implementations. We prove that NRAE is quasi-convex, and thus shares the same global and local optimum with RAE. Moreover, we show the lower-bound of its performance is as good as L_p -norm error when the convexity index satisfies a constraint, which theoretically supports the ANRAT method proposed in the next section.

2.1 Risk-averting Error Criterion

Given training samples $\{\mathbf{X}, y\} = \{(\mathbf{x}_1, y_1), (\mathbf{x}_2, y_2), \dots, (\mathbf{x}_m, y_m)\}$, $f(\mathbf{x}_i, \mathbf{W})$ is the learning model with parameters \mathbf{W} . The loss function of L_p -norm error is defined as:

$$l_p(f(\mathbf{x}_i, \mathbf{W}), y_i) = \frac{1}{m} \sum_{i=1}^m \|f(\mathbf{x}_i, \mathbf{W}) - y_i\|^p \quad (1)$$

When $p = 2$, Eqn. 1 denotes to the standard Mean Square Error (MSE). The Risk-Averting Error criterion (RAE) corresponding to the L_p -norm error is defined by

$$RAE_{p,q}(f(\mathbf{x}_i, \mathbf{W}), y_i) = \frac{1}{m} \sum_{i=1}^m e^{\lambda^q \|f(\mathbf{x}_i, \mathbf{W}) - y_i\|^p} \quad (2)$$

λ is the convexity index. It controls the size of the convexity region.

Because RAE has the sum-exponential form, its Hessian matrix is tuned exactly by the convexity index λ^q . The following theorem indicates the relation between the convexity index and its convexity region.

Theorem 1 (Convexity). *Given the Risk-Averting Error criterion $RAE_{p,q}$ ($p, q \in \mathcal{N}^+$), which is twice continuous differentiable. $J_{p,q}(\mathbf{W})$ and $H_{p,q}(\mathbf{W})$ are the corresponding Jacobian and Hessian matrix. As $\lambda \rightarrow \pm\infty$, the convexity region monotonically expands to the entire parameter space except for the subregion $S := \{W \in \mathcal{R}^n | \text{rank}(H_{p,q}(\mathbf{W})) < n, H_{p,q}(\mathbf{W}) < 0\}$.*

Please refer to the supplementary material for the proof. Intuitively, the use of the RAE was motivated by its emphasizing large individual deviations in approximating functions and optimizing parameters in an exponential manner, thereby avoiding such large individual deviations and achieving robust performances. Theoretically, Theorem 1 states that when the convexity index λ increases to infinity, the convexity region in the parameter space of RAE expands monotonically to the entire space except the intersection of a finite number of lower dimensional sets. The number of sets increases rapidly as the number m of training samples increases. Roughly speaking, larger λ and m cause the size of the convexity region to grow larger respectively in the error space of RAE.

Consider that e^x is a monotonically increasing function, thus RAE shares the same local and global optimum with the standard L_p -norm error. When $\lambda \rightarrow \infty$, the error space can be perfectly stretched to be strictly convex, thus avoid the local optimum to guarantee a global optimum. Although RAE works well in theory, it is not bounded and suffers from the exponential magnitude and arithmetic overflow when using gradient descent in implementations .

2.2 Normalized Risk-Averting Error Criterion

RAE ensures the convexity of the error space to find the global optimum. By using NRAE, we relax the global optimum problem by finding a better local optimum to meet a theoretically and practically reasonable trade-off in real applications.

Given training samples $\{\mathbf{X}, y\} = \{(\mathbf{x}_1, y_1), (\mathbf{x}_2, y_2), \dots, (\mathbf{x}_m, y_m)\}$, $f(\mathbf{x}_i, \mathbf{W})$ is the learning model with parameters W . The Normalized Risk-Averting Error Criterion (NRAE) corresponding to the L_p -norm error is defined as:

$$\begin{aligned} NRAE_{p,q}(f(\mathbf{x}_i, \mathbf{W}), y_i) &= \frac{1}{\lambda^q} \log RAE_{p,q}(f(\mathbf{x}_i, \mathbf{W}), y_i) \\ &= \frac{1}{\lambda^q} \log \frac{1}{m} \sum_{i=1}^m e^{\lambda^q \|f(\mathbf{x}_i, \mathbf{W}) - y_i\|^p} \end{aligned} \quad (3)$$

Theorem 2 (Bounded). *$NRAE_{p,q}(f(\mathbf{x}_i, \mathbf{W}), y_i)$ is bounded.*

The proof is provided in the supplemental materials. Briefly, NRAE is bounded by functions independent of λ and no overflow occurs for $\lambda \gg 1$. The following theorem states the quasi-convexity of NRAE.

Theorem 3 (Quasi-convexity). *Given a parameter space $\{W \in \mathcal{R}^n\}$, Assume $\exists \psi(W)$, s.t. $H_{p,q}(\mathbf{W}) > 0$ when $|\lambda^q| > \psi(W)$ to guarantee the convexity of $RAE_{p,q}(f(\mathbf{x}_i, \mathbf{W}), y_i)$. Then, $NRAE_{p,q}(f(\mathbf{x}_i, \mathbf{W}), y_i)$ is **quasi-convex** and share the same local and global optimum with $RAE_{p,q}(f(\mathbf{x}_i, \mathbf{W}), y_i)$.*

Proof. If $RAE_{p,q}(f(\mathbf{x}_i, \mathbf{W}), y_i)$ is convex, it is quasi-convex. \log function is monotonically increasing, so the composition $\log RAE_{p,q}(f(\mathbf{x}_i, \mathbf{W}), y_i)$ is quasi-convex. ¹

\log is a strictly monotone function and $NRAE_{p,q}(f(\mathbf{x}_i, \mathbf{W}), y_i)$ is quasi-convex, so it shares the same local and global minimizer with $RAE_{p,q}(f(\mathbf{x}_i, \mathbf{W}), y_i)$. \square

¹Because the function f defined by $f(x) = g(U(x))$ is quasi-convex if the function U is quasicconvex and the function g is increasing.

The convexity region of NRAE is consistent with RAE. To interpret this statement in another perspective, the log function is a strictly monotone function. Even if RAE is not strictly convex, NRAE still shares the same local and global optimum with RAE as well as MSE respectively. If we define the mapping function $f : RAE \rightarrow NRAE$, it is easy to see that f is bijective and continuous. Its inverse map f^{-1} is also continuous, so that f is an open mapping. Thus, it is easy to prove that the mapping function f is a homeomorphism to preserve all the topological properties of the given space.

The above theorems state the consistent relations among NRAE, RAE and MSE. It is proven that the greater the convexity index λ , the larger is the convex region is. Intuitively, increasing λ creates tunnels for a local-search minimization procedure to travel through to a good local optimum. However, we care about the justification on the advantage of NRAE against MSE. Theorem 4 provides the theoretical justification for the performance lower-bound of NRAE.

Theorem 4 (Lower-bound). *Given training samples $\{\mathbf{X}, y\} = \{(\mathbf{x}_1, y_1), (\mathbf{x}_2, y_2), \dots, (\mathbf{x}_m, y_m)\}$ and the model $f(\mathbf{x}_i, \mathbf{W})$ with parameters \mathbf{W} . If $\lambda^q \geq 1$, $p, q \in \mathcal{N}^+$ and $p \geq 2$, then both $RAE_{p,q}(f(\mathbf{x}_i, \mathbf{W}), y_i)$ and $NRAE_{p,q}(f(\mathbf{x}_i, \mathbf{W}), y_i)$ always have the better local optimum than the standard L_p -norm error.*

Proof. Let $h_p(\mathbf{W})$ denotes the Hessian matrix of standard L_p -norm error (Eqn. 1), note $\alpha_i(\mathbf{W}) = f(\mathbf{x}_i, \mathbf{W}) - y_i$ we have

$$h_p(\mathbf{W}) = \frac{p}{m} \sum_{i=1}^m \left\{ (p-1) \alpha_i(\mathbf{W})^{p-2} \frac{\partial f(\mathbf{x}_i, \mathbf{W})}{\partial \mathbf{W}} + \alpha_i(\mathbf{W})^{p-1} \frac{\partial^2 f(\mathbf{x}_i, \mathbf{W})}{\partial \mathbf{W}^2} \right\} \quad (4)$$

Since $\lambda^q \geq 1$, let $diag_{eig}$ denotes the diagonal matrix of the eigenvalues from SVD decomposition. \succeq here means 'element-wise greater'. When $A \succeq B$, each element in A is greater than B. Then we have

$$\begin{aligned} diag_{eig}[H_{p,q}(\mathbf{W})] &\succeq diag_{eig} \left[h_p(\mathbf{W}) + \frac{p^2}{m} \sum_{i=1}^m \left\{ \|\alpha_i(\mathbf{W})\|^{2p-2} \frac{\partial f(\mathbf{x}_i, \mathbf{W})}{\partial \mathbf{W}} \right\}^2 \right] \\ &\succeq diag_{eig}[h_p(\mathbf{W})] \end{aligned} \quad (5)$$

This indicates that the $RAE_{p,q}(f(\mathbf{x}_i, \mathbf{W}), y_i)$ always has larger convexity regions than the standard L_p -norm error to better enable escape of local minima. Because $NRAE_{p,q}(f(\mathbf{x}_i, \mathbf{W}), y_i)$ is quasi-convex, sharing the same local and global optimum with $RAE_{p,q}(f(\mathbf{x}_i, \mathbf{W}), y_i)$, the above conclusions are still valid. \square

Roughly speaking, NRAE always has a larger convexity region than the standard L_p -norm error in terms of their Hessian matrix when $\lambda \geq 1$. This property guarantees the higher probability to escape poor local optima using NRAE. In the worst case, NRAE will perform as good as standard L_p -norm error if the convexity region shrinks as λ decreases or the local search deviates from the "tunnel" of convex regions.

More specifically, $NRAE_{p,q}(f(\mathbf{x}_i, \mathbf{W}), y_i)$

- approaches the standard L_p -norm error as $\lambda^q \rightarrow 0$.
- approaches the minimax error criterion $inf_{\mathbf{W}} \alpha_{max}(\mathbf{W})$ as $\lambda^q \rightarrow \infty$.

Please refer to the supplemental materials for the proofs. More rigid proofs that can be generalized to L_p -norm error are also given in [10]. In SimNets, the authors also include quite similar discussions about the robustness with respect to L_p -norm error [13].

3 Learning Methods

We propose a novel learning method to training DNNs with NRAE, called the Adaptive Normalized Risk-Avering Training (ANRAT) approach. Instead of manually tuning λ like GDC [12], we learn λ adaptively in error backpropagation by considering λ as a parameter instead of a hyperparameter. The learning procedure is standard batch SGD. We show it works quite well in theory and practice.

The loss function of ANRAT is

$$l(W, \lambda) = \frac{1}{\lambda^q} \log \frac{1}{m} \sum_{i=1}^m e^{\lambda^q \|f(\mathbf{x}_i, \mathbf{W}) - y_i\|^p} + a \|\lambda\|^{-r} \quad (6)$$

Except for NRAE, we use a penalty term $a \|\lambda\|^{-r}$ to control the changing rate of λ . While minimize the NRAE score, small λ is penalized to regulate the convexity region. a is a hyperparameter to control the penalty index. The first-order derivatives on weight and λ are

$$\frac{dl(W, \lambda)}{dW} = \frac{p \sum_{i=1}^m e^{\lambda^q \alpha_i(W)^{p-1}} \frac{\partial f(\mathbf{x}_i, \mathbf{W})}{\partial \mathbf{W}}}{\sum_{i=1}^m e^{\lambda^q \alpha_i(W)^{p-1}}} \quad (7)$$

$$\frac{dl(W, \lambda)}{d\lambda} = \frac{-q}{\lambda^{q+1}} \log \frac{1}{m} \sum_{i=1}^m e^{\lambda^q \alpha_i(W)^p} + \frac{q}{\lambda} \frac{\sum_{i=1}^m e^{\lambda^q \alpha_i(W)^p} \alpha_i(W)^p}{\sum_{i=1}^m e^{\lambda^q \alpha_i(W)^p}} - ar \lambda^{-r-1} \quad (8)$$

We make a transformation on Eqn. 8 to better understand the gradient with respect to λ . Note that $k_i = \frac{e^{\lambda^q \alpha_i(W)^p}}{\sum_{i=1}^m e^{\lambda^q \alpha_i(W)^p}}$ is actually performing like a probability ($\sum_{i=1}^m k_i = 1$). Ignoring the penalty term, Eqn. 8 can be formulated as follows:

$$\begin{aligned} \frac{dl(W, \lambda)}{d\lambda} &= \frac{q}{\lambda} \left(\sum_{i=1}^m k_i \alpha_i(\mathbf{W})^p - NRAE \right) \\ &= \frac{q}{\lambda} \left(\mathbb{E}(\alpha(\mathbf{W})^p) - NRAE \right) \\ &\approx \frac{q}{\lambda} (L_p\text{-norm error} - NRAE) \end{aligned} \quad (9)$$

Note that as $\alpha_i(\mathbf{W})^p$ becomes smaller, the expectation on $\alpha_i(\mathbf{W})^p$ approaches the standard L_p -norm error. Thus, the gradient on λ is approximately the difference between NRAE and the standard L_p -norm error. Because large λ can incur plateaus to prevent NRAE from finding better optima using SGD [12], they need GDC to gradually deconvexify the NRAE to make the error space well shaped and stable. Through Eqn. 9, ANRAT solve this problem in a more flexible and adaptive manner. When NRAE is larger, Eqn. 9 remains negative and makes λ increase to enlarge the convexity region, facilitating the search in the error space for better optima. When NRAE is smaller, the learned parameters are seemingly going through the optimal "tunnel" for better optima. Eqn. 9 becomes positive to decrease λ and helps NRAE not deviate far from the manifold of the standard L_p -norm error to make the error space stable without large plateaus. Thus, ANRAT adaptively adjusts the convexity index to find an optimal trade-off between better solutions and stability.

This training approach has more flexibility. The gradient on λ as the weighted difference between NRAE and the standard L_p -norm error, enables NRAE to approach the L_p -norm error by adjusting λ gradually. Intuitively, it keeps searching the error space near the manifold of the L_p -norm error to find better optima in a way of competing with and at the same time relying on the standard L_p -norm error space.

In Eqn. 6, the penalty weight a and index r control the convergence speed by penalizing small λ . Smaller a emphasizes tuning λ to allow faster convergence speed between NRAE and L_p -norm error. Larger a forces larger λ for a better chance to find a better local optimum but runs the risk of plateaus and deviating far from the stable error space. r regulates the magnitude of λ and its derivatives in gradient descent.

4 Experiments

We present the results from a series of experiments designed on the MNIST and CIFAR-10 datasets to test the effectiveness of ANRAT for visual recognition with DNNs. We did not explore the full

Table 1: Test set misclassification rates of the best methods that utilized convolutional networks on standard MNIST dataset without data augmentation.

Method	Error %
ConvNets + Stochastic pooling + dropout [18]	0.47
ConvNets + Maxout + dropout [4]	0.45
ConvNets (Lenet-5) [15]	0.95
ConvNets + MSE/CE (this paper)	0.93
large ConvNets, random feature [19]	0.89
ConvNets + L-BFGS [5]	0.69
large ConvNets, hierarchical unsup pretraining [19]	0.62
ConvNets, unsup pretraining, sparsifying logistic [20]	0.6
ConvNets + dropout [18]	0.55
large ConvNets, unsup pretraining [21]	0.53
ConvNets + ANRAT (This paper)	0.52

hyperparameter in Eqn. 6. Instead we fix the hyperparameter at $p = 2$, $q = 2$ and $r = 1$ to mainly compare with MSE. So the final loss function of ANRAT we optimized is

$$l(W, \lambda) = \frac{1}{\lambda^2} \log \frac{1}{m} \sum_{i=1}^m e^{\lambda^2 \|f(\mathbf{x}_i, \mathbf{W}) - y_i\|^2} + a|\lambda|^{-1} \quad (10)$$

This loss function is minimized by batch SGD without complex methods, such as momentum, adaptive/hand tuned learning rates or tangent prop. The learning rate and penalty weight a are selected in $\{1, 0.5, 0.1\}$ and $\{1, 0.1, 0.001\}$ on validation sets respectively. The initial λ is fixed at 10. We use the hold-out validation set to select the best model, which is used to make predictions on the test set. All experiments are implemented quite easily in Python and Theano to obtain GPU acceleration [14].²

The MNIST dataset [15] consists of hand written digits 0-9 which are 28x28 in size. There are 60,000 training images and 10,000 testing images in total. We use 10000 images in training set for validation to select the hyperparameters and report the performance on the test set. We test our method on this dataset without data augmentation.

The CIFAR-10 dataset [16] is composed of 10 classes of natural images. There are 50,000 training images in total and 10,000 testing images. Each image is an RGB image of size 32x32. For this dataset, we adapt pylearn2 [17] to apply the same global contrast normalization and ZCA whitening as was used by Goodfellow et. al [4]. We use the last 10,000 images of the training set as validation data for hyperparameter selection and report the test accuracy.

5 Results and Discussion

5.1 Results on ConvNets

On the MNIST dataset we use the same structure of LeNet5 with two convolutional max-pooling layers but followed by only one fully connected layer and a densely connected softmax layer. The first convolutional layer has 20 feature maps of size 5×5 and max-pooled by 2×2 non-overlapping windows. The second convolutional layer has 50 feature maps with the same convolutional and max-pooling size. The fully connected layer has 500 hidden units. An l_2 prior was used with the strength 0.05 in the Softmax layer. Trained by ANRAT, we can obtain a test set error of 0.52%, which is the best result we are aware of that does not use dropout on the pure ConvNets. We summarize the best published results on the standard MNIST dataset in Table. 1.

²The demo codes, although need to be cleaned and well commented, are published in advance at <https://www.dropbox.com/sh/sb1lp6awt3spyu0/AABv-AHzUObn9YReEjMCafM3a?dl=0>

Table 2: Test accuracy of the best methods that utilized convolutional framework on CIFAR-10 dataset without data augmentation.

Method	Accuracy %
Tiled ConvNets [1]	66.10
Deep Tiled ConvNets + Fine tuning [1]	73.1
ConvNets + Stochastic pooling + dropout [18]	84.87
ConvNets + Local normalization + Max norm + dropout +Bayesian hyperopt [3]	87.39
ConvNets + Maxout + dropout [4]	88.32
ConvNets + MSE + dropout (this paper)	80.58
ConvNets + CE + dropout [18]	80.6
ConvNets + VQ unsup pretraining + feature grouping [2]	82
ConvNets + ANRAT + dropout (This paper)	82.12

The best performing neural networks for pure ConvNets that does not use dropout or unsupervised pretraining achieve an error of about 0.69% [5]. They demonstrated this performance with L-BFGS. Using dropout, ReLU and a response normalization layer, the error reduces to 0.55% [18]. Prior to that, Jarrett et. al showed by increasing the size of the network and using unsupervised pretraining, they can obtain a better result at 0.53% [21]. Using batch SGD to optimize either CE or MSE on the ConvNets described above, we can get an error rate at 0.93%. Replacing the training methods with ANRAT using batch SGD leads to a sharply decreased validation error of 0.66% with a test error at 0.52%. This is the best result among 10 runs, with mean performance of $0.571\% \pm 0.028\%$. This is the best result ever report with pure ConvNets. We also provide an overview of the state of the art achieved by different variants and tricks of DNNs in Table. 1. Even using pure ConvNets and batch SGD, our result is still among the state of the art. Please see more detailed experiments and results in the supplemental materials.

Our next experiment is performed on the CIFAR-10 dataset. We observed significant overfitting using both MSE and ANRAT with the fixed learning rate and batch SGD, so dropout is applied to prevent the co-adaption of weights and improve generalization. We use a similar network layout as in [3] but with only two convolutional max-pooling layers. The first convolutional layer has 96 feature maps of size 5×5 and max-pooled by 2×2 non-overlapping windows. The second convolutional layer has 128 feature maps with the same convolutional and max-pooling size. The fully connected layer has 500 hidden units. Dropout was applied to all the layers of the network with the probability of retaining a hidden unit being $p = (0.9, 0.75, 0.5, 0.5, 0.5)$ for the different layers of the network. Using batch SGD to optimize CE on the simple configuration of ConvNets + dropout, a test accuracy of 80.6 % is achieved [22]. We also reported the performance at 80.58% with MSE instead of CE with the similar network layout. Replacing the training methods with ANRAT using batch SGD gives a test accuracy of 82.12%. This is superior to the results obtained by MSE/CE and competitive with the approach using unsupervised pretraining. The mean of 10 runs is $81.72\% \pm 0.029\%$. In Table. 2, our result is shown to be competitive to those achieved by different ConvNet variants.

5.2 Results on Multilayer Perceptron

On the MNIST dataset, MLPs with unsupervised pretraining has been well studied in recent years, so we select this dataset to compare ANRAT in shallow and deep MLPs with MSE/CE and unsupervised pretraining. For the shallow MLPs, we follow the network layout as in [11, 15] that has only one hidden layer with 300 neurons. We build the stacked architecture and deep network using the same architecture as [23] with 500, 500 and 2000 hidden units in the first, second and third layers, respectively. The training approach is purely batch SGD with no momentum or adaptive learning rate. No weight decay or other regularization technique is applied in our experiments.

Experiment results in Table. 3 show that the deep MLP classifier trained by the ANRAT method has the lowest test error rate (1.55%) of benchmark MLP classifiers with MSE/CE under the same settings. It indicates that ANRAT has the ability to provide reasonable solutions with different initial weight vectors. This result is also better than deep MLP + supervised pretraining or Stacked Logistic Regression networks. We note that the deep MLP using unsupervised pretraining (auto-encoders

Table 3: Test error rate of deep/shallow MLP with different training techniques.

Method	Error %
Deep MLP + supervised pretraining [23]	2.04
Stacked Logistic Regression Network [23]	1.85
Stacked Auto-encoder Network [23]	1.41
Stacked RBM Network [23]	1.2
<hr/>	
Shallow MLP + MSE [15]	4.7
Shallow MLP + GDC [11]	2.7 ± 0.03
Shallow MLP + MSE (this paper)	2.02
Shallow MLP + ANRAT (this paper)	1.94
Shallow MLP + CE [23]	1.93
<hr/>	
Deep MLP + CE [23]	2.4
Deep MLP + MSE (this paper)	1.91
Deep MLP + ANRAT (this paper)	1.55

or RBMs) remains to be the best with test error at 1.41% and 1.2%. Unsupervised pretraining is effective in initializing the weights to obtain a better local optimum. Compared with unsupervised pretraining + fine tuning, ANRAT sometimes still fall into the slightly worse local optima in this case. However, ANRAT is significantly better than MSE/CE without unsupervised pretraining.

Interestingly, we do not observe significant advantages with ANRAT in shallow MLPs. Although in early literature, the error rate on shallow MLPs were reported as 4.7% [15] and 2.7% with GDC [11], both recent papers using CE [23] and our own experiments with MSE can achieve error rate of 1.93% and 2.02%, respectively. Trained by ANRAT, we can have a test rate at 1.94%. This performance is slightly better than MSE, but it is statistically identical to the performance obtained by CE.³ One possible reason is that in shallow networks which can be trained quite well by standard back propagation with normalized initializations, the local optimum achieved with MSE/CE is quite nearly a global optimum or good saddle point. Our result is also corresponding to the conclusion in [6], in which Dauphin et al. extend previous findings on networks with a single hidden layer to show theoretically and empirically that most badly suboptimal critical points are saddle points. Even with better convexity property, ANRAT is as good as MSE/CE in shallow MLPs. However, we find that the problem of poor local optimum becomes more manifest in deep networks. It is easier for ANRAT to find a way towards the better optimum near the manifold of MSE. For the sake of space, please refer to supplemental materials for the results on the shallow Denoised Auto-encoder. The conclusion is consistent that ANRAT performs better when attacking more difficult learning/fitting problems. While ANRAT is slightly better than CE/MSE + SGD on DA with uniform masking noise, it achieves a significant performance boost when Gaussian block masking noise is applied.

6 Conclusions and Outlook

In this paper, we introduce a novel approach, Adaptive Normalized Risk-Averting Training (ANRAT), to help train deep neural networks. Our goal is to demonstrate the effectiveness of ANRAT in both theory and practice. Theoretically, we prove the effectiveness of Normalized Risk-Averting Error on its arithmetic bound, global convexity and local convexity lower-bounded by standard L_p -norm error when convexity index $\lambda \geq 1$. By analyzing the gradient on λ , we explained the reason why using back propagation on λ works. The experiments on deep/shallow network layouts demonstrate comparable or better performance with the same experimental settings among pure ConvNets and MLP + batch SGD on MSE and CE (with or without dropout). Other than unsupervised pretraining, it provides a new perspective to theoretically and practically address the non-convex optimization strategy in DNNs.

Finally, while these early results are very encouraging, clearly further research is warranted to address the questions that arise from non-convex optimization in deep neural networks. It is pre-

³in [23], the author do not report their network settings of the shallow MLP + CE, which may differ from 784-300-10.

liminarily showed that in order to generalize to a wide array of tasks, unsupervised and semi-supervised learning using unlabeled data is crucial. One interesting future work is to take advantage of unsupervised/semi-supervised pretraining with the non-convex optimization methods to train deep neural networks by finding the nearly global optimum. Another crucial question is to guarantee the generalization capability by preventing overfitting. Finally, we are quite interested in generalizing our approach to recurrent neural networks. We leave as future work any performance improvement on benchmark datasets by considering the cutting-edge approach to improve training and generalization performance such as Bayesian hyperparameter optimization, network layout variants, Maxout or SFN, etc.

7 Supplemental Material

7.1 Theoretical Justification

Given training samples $\{\mathbf{X}, y\} = \{(\mathbf{x}_1, y_1), (\mathbf{x}_2, y_2), \dots, (\mathbf{x}_m, y_m)\}$, $f(\mathbf{x}_i, \mathbf{W})$ is the learning model with parameters \mathbf{W} . The Risk-averting Error criterion (RAE) corresponding to the L_p -norm error is defined by

$$RAE_{p,q}(f(\mathbf{x}_i, \mathbf{W}), y_i) = \frac{1}{m} \sum_{i=1}^m e^{\lambda^q \|f(\mathbf{x}_i, \mathbf{W}) - y_i\|^p} \quad (11)$$

The Normalized Risk-averting Error Criterion (NRAE) corresponding to the L_p -norm error is defined as:

$$\begin{aligned} NRAE_{p,q}(f(\mathbf{x}_i, \mathbf{W}), y_i) &= \frac{1}{\lambda^q} \log RAE_{p,q}(f(\mathbf{x}_i, \mathbf{W}), y_i) \\ &= \frac{1}{\lambda^q} \log \frac{1}{m} \sum_{i=1}^m e^{\lambda^q \|f(\mathbf{x}_i, \mathbf{W}) - y_i\|^p} \end{aligned} \quad (12)$$

For clarity, we write the matrix derivatives as function form. In our proof we use quadratic form.

The Jacobian matrix of Eqn. 11 is

$$J_{p,q}(\mathbf{W}) = \frac{1}{m} p \lambda^q \sum_{i=1}^m e^{\lambda^q \|f(\mathbf{x}_i, \mathbf{W}) - y_i\|^p} \|f(\mathbf{x}_i, \mathbf{W}) - y_i\|^{p-1} \frac{\partial f(\mathbf{x}_i, \mathbf{W})}{\partial \mathbf{W}} \quad (13)$$

The Hessian matrix of Eqn. 11 is

$$H_{p,q}(\mathbf{W}) = \frac{p}{m} \sum_{i=1}^m e^{\lambda^q (f(\mathbf{x}_i, \mathbf{W}) - y_i)^p} \quad (14)$$

$$\times \left\{ (p-1) \lambda^q \|f(\mathbf{x}_i, \mathbf{W}) - y_i\|^{p-2} \frac{\partial f(\mathbf{x}_i, \mathbf{W})}{\partial \mathbf{W}} \right\}^2 \quad (15)$$

$$+ p \lambda^{2q} (y_i - f(\mathbf{x}_i, \mathbf{W}))^{2p-2} \frac{\partial f(\mathbf{x}_i, \mathbf{W})}{\partial \mathbf{W}} \right\}^2 \quad (16)$$

$$+ \lambda^q (y_i - f(\mathbf{x}_i, \mathbf{W}))^{p-1} \frac{\partial f^2(\mathbf{x}_i, \mathbf{W})}{\partial \mathbf{W}^2} \} \quad (17)$$

Theorem 5 (Convexity). *Given the Risk-averting Error criterion $RAE_{p,q}$ ($p, q \in \mathcal{N}^+$), which is twice continuous differentiable. $J_{p,q}(\mathbf{W})$ and $H_{p,q}(\mathbf{W})$ are the corresponding Jacobian and Hessian matrix. As $\lambda \rightarrow \pm\infty$, the convexity region monotonically expands to the entire parameter space except for the subregion $S := \{\mathbf{W} \in \mathcal{R}^n | \text{rank}(H_{p,q}(\mathbf{W})) < n, H_{p,q}(\mathbf{W}) < 0\}$.*

Proof. Assume $p > 0$ and $q > 0$, matrix 14 is positive semi-definite. Note that both $\frac{\partial f(\mathbf{x}_i, \mathbf{W})}{\partial \mathbf{W}}$ and $\lambda^{2q} (y_i - f(\mathbf{x}_i, \mathbf{W}))^{2p-2}$ are positive semi-definite, matrix 16 is semi-positive definite, but Eqn. 15 and 17 may be indefinite. Let $\alpha_i(\mathbf{W}) = f(\mathbf{x}_i, \mathbf{W}) - y_i$, We rewrite Eqn. 16 in quadratic form:

$$= p \lambda^{2q} \alpha_i(\mathbf{W})^T \frac{\partial f(\mathbf{x}_i, \mathbf{W})}{\partial \mathbf{W}} \cdot \frac{\partial f(\mathbf{x}_i, \mathbf{W})}{\partial \mathbf{W}} \alpha_i(\mathbf{W}) \quad (18)$$

$$= p \lambda^{2q} \alpha_i(\mathbf{W})^T Q \Lambda Q^T \alpha_i(\mathbf{W}) \quad (19)$$

$$= p \lambda^{2q} S(\mathbf{W})^T \Lambda S(\mathbf{W}) \quad (20)$$

$\Lambda = \text{diag}[\Lambda_1, \Lambda_2, \dots, \Lambda_m]$. Note that when p is an even number, Eqn. 15 is also positive semi-definite.

If $S(\mathbf{W})$ is a full-rank matrix, then Eqn. 20 is positive definite. When $\lambda^q \rightarrow \pm\infty$, the eigenvalues Λ becomes dominant in the leading principal minors (as well as eigenvalues) of the Hessian matrix to make $H_{p,q}(\mathbf{W})$ monotonically increasing with λ^q . Assume $P_\lambda := \{W \in \mathcal{R}^n | H_{p,q}(\mathbf{W}) > 0\}$, we have $P_{\lambda_1} \subseteq P_{\lambda_2}$ when $\lambda_1 < \lambda_2$. Considering Eqn. 15, 16 and 17 are all bounded, $\exists \psi(W)$, s.t. $H_{p,q}(\mathbf{W}) > 0$ when $|\lambda^q| > \psi(W)$.

When $S(\mathbf{W})$ is not a full-rank matrix, the determinant of all its $\binom{n}{k}$ submatrices is 0. Thus, in the subregion $S := \{W \in \mathcal{R}^n | \text{rank}(H_{p,q}(\mathbf{W})) < n, H_{p,q}(\mathbf{W}) < 0\}$, there is no parameters satisfied the convexity conditions ($\bigcup P_\lambda$). \square

Theorem 6 (Bounded). $NRAE_{p,q}(f(\mathbf{x}_i, \mathbf{W}), y_i)$ is bounded.

Proof. Let

$$\alpha_i(\mathbf{W}) = f(\mathbf{x}_i, \mathbf{W}) - y_i \quad (21)$$

$$\alpha_{max}(\mathbf{W}) = \max\{\alpha_i(\mathbf{W}), i = 1, \dots, m\} \quad (22)$$

$$\beta_i(\mathbf{W}) = e^{\lambda^q(|\alpha_{max}(\mathbf{W})|^p - |\alpha_i(\mathbf{W})|^p)} \quad (23)$$

Then we can write Eqn. 12 as

$$\begin{aligned} NRAE_{p,q}(f(\mathbf{x}_i, \mathbf{W}), y_i) &= \frac{1}{\lambda^q} \log \frac{1}{m} e^{\lambda^q |\alpha_{max}|^p} \sum_{i=1}^m \beta_i(\mathbf{W}) \\ &= -\frac{1}{\lambda^q} \log m + |\alpha_{max}|^p + \frac{1}{\lambda^q} \log \sum_{i=1}^m \beta_i(\mathbf{W}) \end{aligned} \quad (24)$$

$$\begin{aligned} &\leq -\frac{1}{\lambda^q} \log m + |\alpha_{max}|^p + \frac{1}{\lambda^q} \log m \cdot e^{\lambda^q |\alpha_{max}|^p} \\ &= 2|\alpha_{max}|^p \end{aligned} \quad (25)$$

\square

More specifically, $NRAE_{p,q}(f(\mathbf{x}_i, \mathbf{W}), y_i)$

- approaches to the standard L_p -norm error as $\lambda^q \rightarrow 0$.
- approaches to the minimax error criterion $\inf_{\mathbf{W}} \alpha_{max}(\mathbf{W})$ as $\lambda^q \rightarrow \infty$.

Intuitively, when $\lambda^q \rightarrow \infty$, we can roughly draw the second conclusion based on Eqn. 24. When $\lambda^q \rightarrow 0$, we have ⁴

$$\begin{aligned} NRAE_{p,q}(f(\mathbf{x}_i, \mathbf{W}), y_i) &= \frac{1}{\lambda^q} \log \frac{1}{m} \sum_{i=1}^m e^{\lambda^q \|f(\mathbf{x}_i, \mathbf{W}) - y_i\|^p} \\ &= \frac{1}{\lambda^q} \log \left(1 + \frac{1}{m} \sum_{i=1}^m \lambda^q \|f(\mathbf{x}_i, \mathbf{W}) - y_i\|^p + O(\lambda^{2q}) \right) \\ &= \frac{1}{m} \sum_{i=1}^m \|f(\mathbf{x}_i, \mathbf{W}) - y_i\|^p \end{aligned} \quad (26)$$

7.2 Experiment Results and Discussions

7.2.1 ConvNets on MNIST

On MNIST dataset, we use the same structure of LeNet5 with two convolutional max-pooling layers followed by a fully connected layer and a densely connected softmax layer. The first convolutional layer has 20 feature maps of size 5×5 and max-pooled by 2×2 non-overlapping windows. The

⁴Consider the rules $e^x = 1 + x + \frac{x^2}{2} + \dots (x \rightarrow 0)$ and $\log x = x - \frac{x^2}{2} + \dots (x \rightarrow 0)$

Table 4: Test set misclassification rates of the best methods that utilized convolutional framework on standard MNIST dataset without data augmentation. Our approach achieves the state-of-the-art result among the algorithms that use standard ConvNets.

Method	Error %
Convolutional DBN [24]	0.82
Convolutional NIN + dropout [25]	0.47
ConvNets + Stochastic pooling + dropout [18]	0.47
ConvNets + Maxout + dropout [4]	0.45
Convolutional Kernel Networks + L-BFGS-B [26]	0.39
Deeply Supervised Nets (DSN-L2SVM) + dropout [27]	0.39
ConvNets (Lenet-5) [15]	0.95
ConvNets + MSE/CE (this paper)	0.93
large ConvNets, random feature [19]	0.89
ConvNets + L-BFGS [5]	0.69
large ConvNets, hierarchical unsup pretraining [19]	0.62
ConvNets, unsup pretraining, sparsifying logistic [20]	0.6
ConvNets + dropout [18]	0.55
large ConvNets, unsup pretraining [21]	0.53
ConvNets + ANRAT (This paper)	0.52

second convolutional layer has 50 feature maps with the same convolutional and max-pooling size. The fully connected layer has 500 hidden units. An l_2 prior was used, with strength 0.05 in the Softmax layer on MNIST. Trained by ANRAT, we obtained a test set error of 0.52%, which is the best result we are aware of that does not use dropout on the pure ConvNets. We summarize the best published results on the standard MNIST dataset in Table. 4.

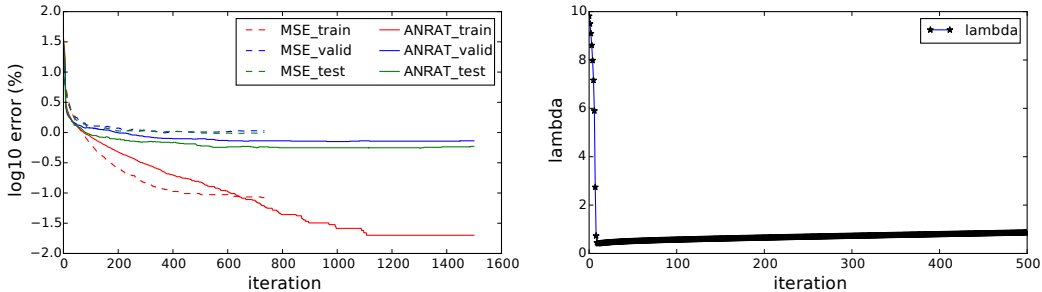


Figure 1: (a). MNIST train, validation and test error rates throughout training with Batch SGD for MSE and ANRAT with l_2 priors. We cross-validated the learning rate and regularization weight on validation set for ConvNets (left). (b). The curve of λ throughout ANRAT training (right).

Using the same network architecture described in the full paper, we trained two ConvNets using MSE and ANRAT respectively and compare their performance. Fig. 1 (a) shows the progression of train, validation and test errors over 160 training epochs. The errors trained on MSE plateau as it can not train the ConvNets sufficiently and underfits. Using ANRAT, the validation and test errors remain decreasing along with the training error. During training, λ sharply decrease, regulating the tunnel of NRAE to approach the manifold of MSE. Afterward the penalty term becomes significant, force λ to grow gradually while expanding the convex region for higher chance to find the better optimum (Fig. 1 (b)).

7.2.2 ConvNets on CIFAR-10

Our next experiment is performed on CIFAR-10 dataset. Since we observed significant overfitting in both MSE and ANRAT with fixed learning rate and batch SGD, dropout is applied to prevent the co-adaptation of weights and improve generalization capability. We use the similar network layout as in

Table 5: Test accuracy of the best methods that utilized convolutional framework on CIFAR-10 dataset without data augmentation. Our approach is superior to MSE/CE + SGD training and competitive with the approach that uses unsupervised pretraining. Our result is also among the state of the art achieved by different variants of DNNs.

Method	Accuracy %
Tiled ConvNets [1]	66.10
Convolutional mcRBM [28]	71
Deep Tiled ConvNets + Fine tuning [1]	73.1
Convolutional Kernel Networks + L-BFGS-B [26]	82.18
ConvNets + Local normalization + Max norm + dropout +Bayesian hyperopt [3]	87.39
ConvNets + Stochastic pooling + dropout [18]	84.87
ConvNets + Maxout + dropout [4]	88.32
Convolutional NIN + dropout [25]	89.6
Deeply Supervised Nets (DSN-L2SVM) + dropout [27]	90.22
<hr/>	
ConvNets + MSE + dropout (this paper)	80.58
ConvNets + CE + dropout [18]	80.6
ConvNets + VQ unsup pretraining + feature grouping [2]	82
ConvNets + ANRAT + dropout (This paper)	82.12

[3] but with only two convolutional max-pooling layers. The first convolutional layer has 96 feature maps of size 5×5 and max-pooled by 2×2 non-overlapping windows. The second convolutional layer has 128 feature maps with the same convolutional and max-pooling size. The fully connected layer has 500 hidden units. Dropout was applied to all the layers of the network with the probability of retaining a hidden unit being $p = (0.9, 0.75, 0.5, 0.5, 0.5)$ for the different layers of the network.

Among 10 experiments trained by ANRAT, we can obtain a test accuracy of 82.12%, which is superior to the results reported in [18] with the similar configurations. We summarize the best published results on the standard CIFAR-10 dataset in Table. 5.

The best performing neural networks for pure ConvNets setting with dropout can achieve a test accuracy of 87.29% [3]. They followed the tricks that applied to solve ILSVRC-2010 ImageNet contest in [22], including local normalization layer, max norm constraint and Bayesian hyperparameter optimization techniques. To control the factor that influence the performance, we did not apply above tricks in our experiments. Fortunately, [18] reported the results with the similar configuration with our experiments. Using batch SGD to optimize either CE on the simple configuration of ConvNets + dropout, a test accuracy of 80.6 % is achieved. We also reported the performance at 80.58% with MSE instead of CE with our network layout. Replacing the training methods to ANRAT using batch SGD leads a test accuracy of 82.12%. This is superior to the results obtained by MSE/CE and competitive with the approach using unsupervised pretraining. The statistics of 10 times running is $81.72\% \pm 0.029\%$. In Table. 5, our result is competitive to those achieved by different ConvNets variants and among the state of the art.

7.3 Results on MLP

While ConvNets leads the state of the art performance on visual recognition, general multilayer perceptron (MLP) is an important framework for generative and discriminative learning. Unsupervised layer-wise pretraining by RBM or auto-encoder demonstrate superb performance boosting on visual recognition with MLP.

on MNIST dataset, MLP with unsupervised pretraining was well studied in recent years, so we select this dataset to compare ANRAT in shallow and deep MLP with MSE/CE and unsupervised pretraining. For the shallow MLP, we follow the network layout as in [11, 15] that has only one hidden layer with 300 neurons. We build the stacked architecture and deep network using the same architecture as [23] with 500, 500 and 2000 hidden units in the first, second and third layers respectively. Training approach is purely batch SGD with no momentum or adaptive learning rate. No weight decay or other regularization technique is applied in our experiments.

Table 6: Test error rate of deep.shallow MLP with different training techniques. Our approach is superior to MSE/CE + SGD training and comparable with the approach that uses unsupervised pretraining.

Method	Error %
Deep MLP + supervised pretraining [23]	2.04
Stacked Logistic Regression Network [23]	1.85
Stacked Auto-encoder Network [23]	1.41
Stacked RBM Network [23]	1.2
<hr/>	
Shallow MLP + MSE [15]	4.7
Shallow MLP + GDC [11]	2.7 ± 0.03
Shallow MLP + MSE (this paper)	2.02
Shallow MLP + ANRAT (this paper)	1.94
Shallow MLP + CE [23]	1.93
<hr/>	
Deep MLP + CE [23]	2.4
Deep MLP + MSE (this paper)	1.91
Deep MLP + ANRAT (this paper)	1.55

Experimental results in Table. 6 show that the deep MLP classifier trained by ANRAT method has the lowest test error rate (1.55%) than benchmark MLP classifiers with MSE/CE with the same settings. It indicates that the ANRAT method has the ability to provide reasonable generalization results with different initial weight vectors. This result are also better than deep MLP + supervised pretraining or Stacked Logistic Regression network. However, we note that the deep MLP using unsupervised pretraining (auto-encoders or RBM) is remaining the best with the test error at 1.41% and 1.2%. Unsupervised pretraining is still effective to better initialize the weight to obtain a better local optimum. Compared with unsupervised pretraining + fine tuning, ANRAT sometimes still fall into the slightly worse local optimum in this case. However, ANRAT is significantly better than MSE/CE without unsupervised pretraining.

Interestingly, we do not observe significant advantages with ANRAT against MSE/CE methods. Although in early literatures, the error rate were reported as 4.7% [15] and 2.7% with GDC [11], both recent paper using shallow MLP + CE [23] and our own experiment with shallow MLP + MSE can achieve the error rate of 1.93% and 2.02% respectively. Trained by ANRAT, we can achieve the test rate of 1.94%. This performance is slightly better than MSE, but it is statistically identical to the performance obtained by CE.⁵ The possible reason is in shallow network which can be trained quite well by standard back propagation, the local optimum achieved with MSE/CE is quite nearly global optimum or good saddle points. Actually this experiment also validate the assumption in [6], in which Dauphin et al. extend previous findings on networks with a single hidden layer to show theoretically and empirically that most badly suboptimal critical points are saddle points. When ANRAT explores the manifold near MSE/CE, more optimal solution is too more implicit to find. The good point is ANRAT is theoretically and empirically guaranteed to be no worse than the L_P -norm error (MSE). Deep network is hard to train and the problem of poor local optimum becomes more manifest. It is easier for ANRAT to find a way towards the better optimum near the manifold of MSE. Moreover, the exponential form of NRAE helps to alleviate vanishing of gradient also help training deep networks.

7.3.1 Results on Denoised Auto-encoder

Our last experiments focus on generative learning instead of discriminative learning. In [29], Denoised Auto-encoder (DA) is well studied to show the ability to learn useful representations. We were considering if ANRAT is likely to lead to the learning of feature detectors that detect better structure in the input patterns with more sufficient training.

⁵in [23], the author do not report their network settings of the shallow MLP + CE, which may differ from 784-300-10.

On MNIST dataset, we use a single-layer DA with the local masking noise at the levels from 30% to 60%. That is, we randomly set the pixels to be 0 evenly. Another noise paradigm is Gaussian block noise. We randomly select centroids to span masking blocks in terms of each centroid with a Gaussian distribution. The noise level differs from 33.3% to 52.6% accordingly. Figure. 2 shows three examples of different corruption level. We train the DA using ANRAT and MSE with pure batch SGD with fixed learning rate among $\{1, 0.1, 0.01\}$ for 1000 epochs and report the best reconstruction MSE.

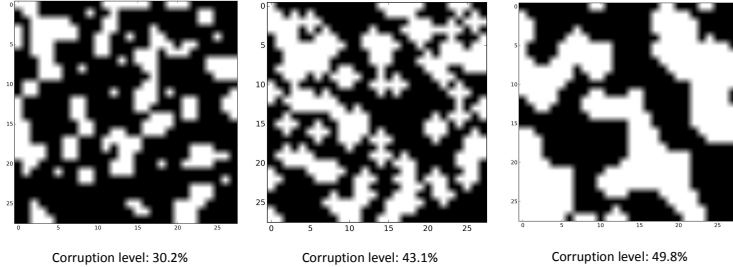


Figure 2: Example maps of Gaussian block masking.

As in the shallow network, we found the advantage of ANRAT is statistically significant in DA but the difference is very small when using masking noise (Figure. 7). Although masking makes it harder to reconstruct original images, the strong spatial correlations are still existed between masked pixels and the "good" pixels nearby, thus helps DA to learn the generative distribution from the conditional probability with respect to the manifold of the added noise. The local optimum found by both SGD training with MSE and ANRAT is nearly optimal. When applying Gaussian block noise as shown in Figure. 2, masking blocks cover several patches instead of scattered points. It is much harder to learn the spatial correlation within the masking areas. On this tougher task, ANRAT performs much better than using batch SGD on MSE. In Figure. 7, the reconstruction MSE using ANRAT on each image is 1.078, which is 24.09% lower than 1.432 obtained by batch SGD on MSE.

Table 7: Reconstruction MSE of DA output trained by ANRAT and MSE error criterion at different masking level using random masking or Gaussian block masking. The mean and standard deviation over 20 times running are reported.

Corruption Level	MSE	ANRAT
30%	4.552 (0.006)	4.348 (0.005)
40%	5.697 (0.007)	5.57 (0.005)
50%	7.112 (0.005)	7.071 (0.007)
60%	9.245 (0.008)	9.1 (0.008)
Gaussian Isotropic Masking (33.3% - 52.6%)	1.432 (0.0002)	1.078 (0.009)

In Figure. 3 (a), the curve of training error using ANRAT penetrates across the curve trained by MSE after several epochs and is consistently staying lower. Note that NRAE and L_P norm can be compared since they are homeomorphism and in the same magnitude, but there is still a "gap" between them. So, λ is still forced to fluctuate, gradually grow larger to find more optimal tunnel towards the better optimum (Figure 3 (b)). This keeps ANRAT searching for better results near the manifold of MSE through a gradual convexing on its convexity region. In Figure. 4, DA using ANRAT learned a lightly more diverse features than SGD on MSE when uniform masking is applied. In the case of Gaussian block masking, DA learned more clear meaningful features with the help of ANRAT.

7.4 Summarization

To summarize, we introduce a novel approach, Adaptive Normalized Risk-Averting Training (ANRAT) to help train the deep neural networks more sufficiently. our goal is to demonstrate the effectiveness of ANRAT in both theory and practice. The experiments on deep/shallow networks layouts

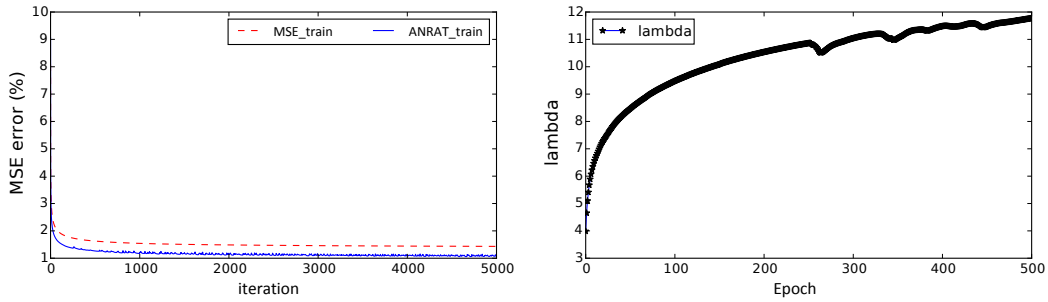


Figure 3: (a). Reconstruction MSE throughout training by Batch SGD for MSE and ANRAT (left). Gaussian block noise is applied at input layer. (b). The curve of λ throughout ANRAT (right).

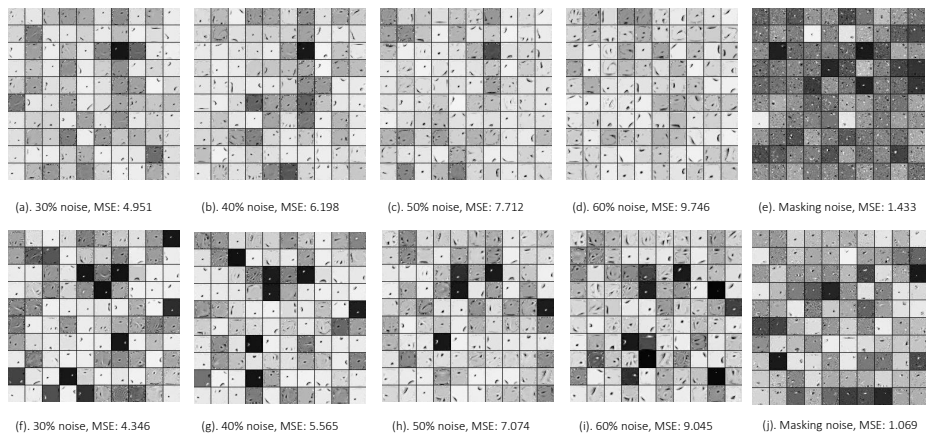


Figure 4: 100 feature maps learned by Denoised Auto-encoder using ANRAT and batch SGD on MSE. Different corruption level of uniform masking and Gaussian block masking are applied at the input layer.

demonstrate comparable or better performance with the same experimental settings among those use pure ConvNets and MLP + batch SGD on MSE and CE (with or without dropout). Other than unsupervised pretraining, It provides a new perspective to theoretically and practically address the non-convex optimization strategy in DNNs. Theoretically, we prove the effectiveness of Normalized Risk-Averting Error on its arithmetic bound, global convexity and local convexity lower-bounded by standard L_p -norm error when convexity index $\lambda \geq 1$. By analyzing the gradient on λ , we explained the reason why using back propagation on λ works.

Empirically, we compare ANRAT with batch SGD training on MSE/CE and unsupervised pretraining using pure ConvNets on MNIST and CIFAR-10 datasets. ANRAT achieves comparable or better performance with the same experiment settings among those use pure ConvNets + batch SGD and/or dropout. An overview of the comparisons among the best results obtained from different training methods and model variants is also provided to validate the performance of ANRAT is among the state of the art. Except for ConvNets, we evaluate ANRAT in shallow/deep multilayer perceptrons. Although the advantage of ANRAT is not significant against CE/MSE + SGD in shallow neural networks, it overtakes CE/MSE + SGD in deep neural networks and approaches to the performance achieved by unsupervised pretraining such as RBM and auto-encoder. To better understand ANRAT on generative models, experiments on shallow Denoised Auto-encoders are also performed with uniform masking noise and Gaussian block masking noise at the input layer. While ANRAT is

slightly better than CE/MSE + SGD on DA with the uniform masking noise, it achieves significant performance boosting when Gaussian block masking noise is applied.

References

- [1] Jiquan Ngiam, Zhenghao Chen, Daniel Chia, Pang W Koh, Quoc V Le, and Andrew Y Ng. Tiled convolutional neural networks. In *Advances in Neural Information Processing Systems*, pages 1279–1287, 2010.
- [2] Adam Coates and Andrew Y Ng. Selecting receptive fields in deep networks. In *Advances in Neural Information Processing Systems*, pages 2528–2536, 2011.
- [3] Nitish Srivastava, Geoffrey Hinton, Alex Krizhevsky, Ilya Sutskever, and Ruslan Salakhutdinov. Dropout: A simple way to prevent neural networks from overfitting. *The Journal of Machine Learning Research*, 15(1):1929–1958, 2014.
- [4] Ian J Goodfellow, David Warde-Farley, Mehdi Mirza, Aaron Courville, and Yoshua Bengio. Maxout networks. *arXiv preprint arXiv:1302.4389*, 2013.
- [5] Jiquan Ngiam, Adam Coates, Ahbik Lahiri, Bobby Prochnow, Quoc V Le, and Andrew Y Ng. On optimization methods for deep learning. In *Proceedings of the 28th International Conference on Machine Learning (ICML-11)*, pages 265–272, 2011.
- [6] Yann N Dauphin, Razvan Pascanu, Caglar Gulcehre, Kyunghyun Cho, Surya Ganguli, and Yoshua Bengio. Identifying and attacking the saddle point problem in high-dimensional non-convex optimization. In *Advances in Neural Information Processing Systems*, pages 2933–2941, 2014.
- [7] Andrew Blake and Andrew Zisserman. *Visual reconstruction*, volume 2. MIT press Cambridge, 1987.
- [8] WB Liu and Christodoulos A Floudas. A remark on the gop algorithm for global optimization. *Journal of Global Optimization*, 3(4):519–521, 1993.
- [9] Jason L Speyer, John Deyst, and D Jacobson. Optimization of stochastic linear systems with additive measurement and process noise using exponential performance criteria. *Automatic Control, IEEE Transactions on*, 19(4):358–366, 1974.
- [10] James Ting-Ho Lo. Convexification for data fitting. *Journal of global optimization*, 46(2):307–315, 2010.
- [11] Yichuan Gui, James Ting-Ho Lo, and Yun Peng. A pairwise algorithm for training multilayer perceptrons with the normalized risk-averting error criterion. In *Neural Networks (IJCNN), 2014 International Joint Conference on*, pages 358–365. IEEE, 2014.
- [12] James Ting-Ho Lo, Yichuan Gui, and Yun Peng. Overcoming the local-minimum problem in training multilayer perceptrons with the nrae training method. In *Advances in Neural Networks–ISNN 2012*, pages 440–447. Springer, 2012.
- [13] Nadav Cohen and Amnon Shashua. Simnets: A generalization of convolutional networks. *arXiv preprint arXiv:1410.0781*, 2014.
- [14] Frédéric Bastien, Pascal Lamblin, Razvan Pascanu, James Bergstra, Ian J. Goodfellow, Arnaud Bergeron, Nicolas Bouchard, and Yoshua Bengio. Theano: new features and speed improvements. Deep Learning and Unsupervised Feature Learning NIPS 2012 Workshop, 2012.
- [15] Yann LeCun, Léon Bottou, Yoshua Bengio, and Patrick Haffner. Gradient-based learning applied to document recognition. *Proceedings of the IEEE*, 86(11):2278–2324, 1998.
- [16] Alex Krizhevsky and Geoffrey Hinton. Learning multiple layers of features from tiny images. *Computer Science Department, University of Toronto, Tech. Rep*, 1(4):7, 2009.
- [17] Ian J Goodfellow, David Warde-Farley, Pascal Lamblin, Vincent Dumoulin, Mehdi Mirza, Razvan Pascanu, James Bergstra, Frédéric Bastien, and Yoshua Bengio. Pylearn2: a machine learning research library. *arXiv preprint arXiv:1308.4214*, 2013.
- [18] Matthew D Zeiler and Rob Fergus. Stochastic pooling for regularization of deep convolutional neural networks. *arXiv preprint arXiv:1301.3557*, 2013.

- [19] M Ranzato, Fu Jie Huang, Y-L Boureau, and Yann LeCun. Unsupervised learning of invariant feature hierarchies with applications to object recognition. In *Computer Vision and Pattern Recognition, 2007. CVPR'07. IEEE Conference on*, pages 1–8. IEEE, 2007.
- [20] Christopher Poultney, Sumit Chopra, Yann L Cun, et al. Efficient learning of sparse representations with an energy-based model. In *Advances in neural information processing systems*, pages 1137–1144, 2006.
- [21] Kevin Jarrett, Koray Kavukcuoglu, M Ranzato, and Yann LeCun. What is the best multi-stage architecture for object recognition? In *Computer Vision, 2009 IEEE 12th International Conference on*, pages 2146–2153. IEEE, 2009.
- [22] Alex Krizhevsky, Ilya Sutskever, and Geoffrey E Hinton. Imagenet classification with deep convolutional neural networks. In *Advances in neural information processing systems*, pages 1097–1105, 2012.
- [23] Hugo Larochelle, Yoshua Bengio, Jérôme Louradour, and Pascal Lamblin. Exploring strategies for training deep neural networks. *The Journal of Machine Learning Research*, 10:1–40, 2009.
- [24] Honglak Lee, Roger Grosse, Rajesh Ranganath, and Andrew Y Ng. Convolutional deep belief networks for scalable unsupervised learning of hierarchical representations. In *Proceedings of the 26th Annual International Conference on Machine Learning*, pages 609–616. ACM, 2009.
- [25] Shuicheng Yan Min Lin, Qiang Chen. Network in network. *arXiv preprint arXiv:1312.4400v3*, 2014.
- [26] Julien Mairal, Piotr Koniusz, Zaid Harchaoui, and Cordelia Schmid. Convolutional kernel networks. In *Advances in Neural Information Processing Systems*, pages 2627–2635, 2014.
- [27] Chen-Yu Lee, Saining Xie, Patrick Gallagher, Zhengyou Zhang, and Zhuowen Tu. Deeply-supervised nets. *arXiv preprint arXiv:1409.5185*, 2014.
- [28] M Ranzato and Geoffrey E Hinton. Modeling pixel means and covariances using factorized third-order boltzmann machines. In *Computer Vision and Pattern Recognition (CVPR), 2010 IEEE Conference on*, pages 2551–2558. IEEE, 2010.
- [29] Pascal Vincent, Hugo Larochelle, Isabelle Lajoie, Yoshua Bengio, and Pierre-Antoine Manzagol. Stacked denoising autoencoders: Learning useful representations in a deep network with a local denoising criterion. *The Journal of Machine Learning Research*, 11:3371–3408, 2010.